Is the Envelope Beneficial to Non-Orthogonal Multiple Access?

Ziyi Xie, *Student Member, IEEE,* Wenqiang Yi, *Member, IEEE,* Xuanli Wu, *Member, IEEE,* Yuanwei Liu, *Senior Member, IEEE,* and Arumugam Nallanathan, *Fellow, IEEE*

Abstract—Non-orthogonal multiple access (NOMA) is capable of serving different numbers of users in the same time-frequency resource element, and this feature can be leveraged to carry additional information. In the orthogonal frequency division multiplexing (OFDM) system, a novel enhanced NOMA scheme called NOMA with informative envelope (NOMA-IE) is proposed to explore extra flexibility from the envelope of NOMA signals. In this scheme, data bits are conveyed by the quantified signal envelope in addition to classic signal constellations. The sub-carrier activation patterns of different users are jointly decided by the envelope former at the transmitter of NOMA-IE. At the receiver, successive interference cancellation (SIC) is employed, and the envelope detection coefficient is introduced to eliminate the error floor. Theoretical expressions of spectral efficiency, energy efficiency, and detection complexity are provided first. Then, considering the binary phase shift keying modulation, the block error rate and bit error rate are derived based on the two-subcarrier element. The analytical results reveal that the SIC error and the index error are the main factors degrading the error performance. The numerical results demonstrate the superiority of the NOMA-IE over the OFDM and OFDM-NOMA, especially in the high signal-to-noise ratio (SNR) regime.

Index Terms—Bit error rate, index modulation, non-orthogonal multiple access, OFDM, successive interference cancellation.

I. INTRODUCTION

Due to emerging Internet-enabled applications, such as extended reality (XR) services and telemedicine, the next-generation wireless networks require a more robust communication quality [2], [3]. Non-orthogonal multiple access (NOMA) has been regarded as a promising multiple access candidate for future networks [4]–[6]. Different from orthogonal multiple access (OMA), multiple users in NOMA can be served by the same time-frequency resource element by utilizing the code or power domain. Particularly in power-domain NOMA, the superposition coding is applied at the transmitter for power multiplexing, and the successive interference cancellation (SIC) is adopted at the receiver for detection. When considering the perfect SIC process and user fairness, it has been theoretically proved that NOMA[1] has a larger sum rate than OMA in high signal-to-noise ratio (SNR) regimes [7]. Recent contributions focused on the Shannon channel capacity evaluation of NOMA in various scenarios [8]–[11]. With the

error-free decoding assumption, it is difficult for the initial NOMA studies to evaluate the communication quality under practical modulation schemes, especially with a non-ideal SIC process.

Another interesting property of NOMA in multi-carrier systems is that the number of users in the same subcarrier is more than one. This quantified signal envelope can be utilized to carry additional information. For example, in the two-user case, all possible numbers of users in a subcarrier are 0, 1, and 2. Therefore, the envelope is able to convey at most $\log_2 3$ bits of information. There is a similar concept called orthogonal frequency division multiplexing with index modulation (OFDM-IM) in the OMA scheme [12]–[14]. OFDM-IM is developed from the orthogonal frequency division multiplexing (OFDM), which has been involved in wireless communication standards since Long Term Evolution (LTE) due to its capability of combating the intersymbol interference caused by the frequency-selective fading channel. In OFDM-IM, if there is no signal in a subcarrier, the subcarrier is inactive; otherwise, it is active. Exploiting the subcarrier orthogonality in conventional OFDM, OFDM-IM introduces a new subcarrier-index dimension to carry information in addition to the classical signal constellations, i.e., those binary subcarrier activation patterns convey additional information [15]–[17]. OFDM-IM has been regarded as an effective scheme providing either bit error rate (BER) performance enhancement or power-efficiency improvement [18], [19]. To explore the potential of the OFDM-IM in multi-user cases, several works have investigated the combination of the OFDM-IM framework and NOMA [20], [21]. However, these works simply applied OFDM-IM waveforms to different NOMA users, and the performance enhancement is under specific conditions. In this work, we propose a novel *NOMA with informative envelope (NOMA-IE)* scheme, where the activation patterns of different users are jointly decided by the transmitter.

A. Related Works

In practical implementation, when considering the finite constellation input, the decoding error cannot be ignored, especially during the SIC process [22]. Therefore, recent research has paid attention to the error probability of link-level NOMA transmissions. The exact closed-form expression of bit error rate (BER) under fading channels was firstly derived in [22], where the binary phase shift keying (BPSK) and quadrature phase shift keying (QPSK) are selected for the far user and the near user, respectively. In [23], the authors provided the exact symbol error rate with arbitrary ordered pulse amplitude modulation (PAM) and quadrature amplitude modulation (QAM).

Z. Xie and X. Wu are with the School of Electronics and Information Engineering, Harbin Institute of Technology, Harbin 150001, China (email: {ziyi.xie, xlwu2002}@hit.edu.cn).

W. Yi, Y. Liu, and A. Nallanathan are with the School of Electronic Engineering and Computer Science, Queen Mary University of London, E1 4NS, U.K. (email: {w.yi, yuanwei.liu, a.nallanathan}@qmul.ac.uk).

[1]In this work, NOMA refers to the power-domain NOMA.

2

Nevertheless, these works are limited to the two-user scenario. The authors in [24] considered the BPSK modulation and investigated the BER performance when the number of users is arbitrary. A NOMA real-time test system was employed to validate the results. Both the asymptotic and exact BER expressions of the QAM with arbitrary modulation order were obtained in multi-user downlink NOMA systems [25].

Some simple combinations of the NOMA concept and OFDM-IM have been studied in previous works. In [26], the authors focused on a hybrid NOMA scheme exploring power domain multiplexing of OFDM and OFDM-IM. The proposed scheme has better error performance and achievable rate than the conventional OFDM-based NOMA. In [20] and [21], all NOMA users adopt the OFDM-IM for downlink transmissions, and the scheme is termed IM-NOMA. Different user requirements can be fulfilled by adjusting power allocation factors and subcarrier activation ratios. In [27], the uplink NOMA was considered, and the OFDM-IM was proved to reduce the impact of the collision on the ultrareliable low-latency communication. In the above works, data bits of NOMA users are mapped to subcarrier activation patterns separately before the superposition coding, and the envelopes of different signals are independent. As summarized in Table I, however, the current integration of NOMA and OFDM-IM brings problems in terms of theoretical performance analysis and practical realization. For tractability, the previous works derived the approximated BER expressions by ignoring the interference caused by NOMA but treating it as noise. In addition, the detection error floor occurs when applying the OFDM-IM framework, which degrades the error performance when similar power levels are allocated to different NOMA users [28].

B. Motivations and Contributions

As we have discussed, although the OFDM-IM framework has the potential to leverage the signal envelope as a new degree of freedom to boost the performance of NOMA, multiple problems emerge when simply combining the two techniques. In this work, considering practical modulation schemes, a novel NOMA-IE design is proposed. In this scheme, we jointly design the subcarrier activation patterns for each user, and hence the envelope of the superposed signal conveys information. More specifically, we aim at answering the following questions:

- **Question 1**: How to derive accurate BER expressions of NOMA-IE with the consideration of intra-cluster interference in NOMA?
- **Question 2**: How to reduce or eliminate the detection error floor?
- **Question 3**: With the additional flexibility from the envelope, how does the performance superiority of NOMA-IE over conventional OFDM or OFDM-NOMA behave?

We provide a detailed analysis and discussion of the proposed NOMA-IE. The main contributions of this paper are summarized as follows:

- We propose a novel NOMA-IE scheme based on the OFDM-IM framework in downlink transmissions and take the two-user case as an example. At the transmitter,

we employ an envelope former module to jointly decide the subcarrier activation patterns of two NOMA users. At the receiver, we adopt the SIC process as in conventional NOMA systems. We introduce the envelope detection coefficient to the signal detection procedure.

- We provide a brief analysis of spectral efficiency, energy efficiency, and detection complexity. Then we mainly focus on the theoretical block error rate (BLER) and BER performance of the proposed NOMA-IE, where intra-cluster interference and imperfect SIC process are considered. By splitting the multi-subcarrier OFDM subblock into multiple two-subcarrier elements (TSEs), we derive the BLER and BER expressions with BPSK modulation for two NOMA users to answer **Question 1**. The analytical results show that the SIC error and the index error significantly degrade the error performance.

- We illustrate that the value of the power allocation coefficient affects the detection error floor when employing the detection method in previous works. Since the design of NOMA-IE avoids the constellation overlap in NOMA signals, we eliminate the detection error floor in NOMA-IE by adjusting the envelope detection coefficient, and **Question 2** is answered. We also show that an appropriate envelope detection coefficient value helps to achieve low error probability.

- We answer **Question 3** by numerical results. The numerical results validate our analysis and demonstrate that: 1) compared with the conventional OFDM, the NOMA-IE reduces the error probability with a wide range of power allocation coefficients; 2) NOMA-IE with the feasible envelope detection coefficient has better error performance than IM-NOMA in most cases; 3) under equal spectral efficiency and energy efficiency, the proposed NOMA-IE outperforms OFDM-NOMA, especially at a high SNR.

The rest of the paper can be summarized as follows. In Section II, the system model of NOMA-IE is presented. In Section III, we provide a preliminary analysis including spectral efficiency, energy efficiency, and detection complexity. The theoretical error probabilities of NOMA-IE are investigated in Section IV. In Section V, numerical results are illustrated. Finally, Section VI concludes the paper.

Notation: $(\cdot)^T$ denotes the transpose operation. $|\cdot|$ denotes the absolute value if applied to a complex number or the cardinality if applied to a set. $\|\cdot\|$ denotes the Frobenius norm. $\binom{n}{k} = \frac{n!}{k!(n-k)!}$ denotes the binomial coefficient and $\lfloor \cdot \rfloor$ is the floor function. $Q(\cdot)$ denotes the Gaussian Q-function. The probability of an event is denoted by $\Pr(\cdot)$. $\det(\mathbf{A})$ stands for the rank of $\mathbf{A}$. $\mathbf{I}_N$ is the identity matrix with the dimension $N \times N$. For the vector $\mathbf{x} = [x(1), x(2), ..., x(n)]^T$, we define $\mathbf{X} = \mathrm{diag}\{x(1), x(2), ..., x(n)\}$. $X \sim \mathcal{CN}(0, \sigma^2)$ represents the distribution of a circularly symmetric complex Gaussian random variable X with variance σ^2.

II. SYSTEM MODEL

As shown in Fig. 1, we consider a downlink NOMA-IE scheme based on the OFDM-IM framework, where a near user (NU) and a far user (FU) share total N_T subcarriers.

TABLE I
A SUMMARY OF RELATED WORKS ON NOMA IN OFDM-IM FRAMEWORK

Reference	System Setup	NOMA Interference	Detection Error Floor
[27], [28]	Uplink	Ignored	Always exist
[20], [21]	Downlink	Ignored	Exist in a range of power allocation coefficients
[26]	Downlink	Ignored	Eliminate by design of hybrid OFDM and OFDM-IM
This work	Downlink	Considered	Eliminate by design of informative envelope

This system operates in a Rayleigh fading environment, and the fading gains on different subcarriers are independent and identically distributed.

A. Transmitter Design with Envelope Forming

In NOMA-IE, the total N_T OFDM subcarriers are divided into $G = N_T/L$ subblocks, each of which consists of L subcarriers as shown in Fig. 1(b). Thus data bits of both users are equally split into G groups for transmission. In each data group, part of the data bits called index bits is for the decision on the active subcarrier indices while the other part called symbol bits is modulated on active subcarriers. For subblock $g \in \{1, 2, ..., G\}$, we use $\mathbf{I}_{g,u}$ to denote the indices set of active subcarriers, where $u \in \{N, F\}$.

Assumption 1. *(Principle of Envelope Forming) In the NOMA-IE scheme, the set of active subcarriers for the NU is a subset of that for the FU, i.e., $\mathbf{I}_{g,N} \subseteq \mathbf{I}_{g,F}$*[2].

The number of active subcarriers $K_{g,u}$ in the subblock g is the cardinality of $\mathbf{I}_{g,u}$, i.e., $K_{g,u} = |\mathbf{I}_{g,u}|$, and hence $K_{g,N} \le K_{g,F} \le L$ holds.

Remark 1. *The special cases of the NOMA-IE are other classic OFDM-based schemes. When $K_{g,N} = 0$ and $K_{g,F} = L$, the NOMA-IE becomes the conventional OFDM. When $K_{g,N} = 0$ and $0 < K_{g,F} < L$, the NOMA-IE is the OFDM-IM. When $K_{g,N} = K_{g,F} = L$, it can be regarded as the OFDM-NOMA [29].*

Since data bits conveyed by different subblocks are independent, we focus on one subblock in the rest of the paper, and we denote $K_{g,u} = K_u$, where K_u is a constant. As the calculation in OFDM-IM [16], when employing the M_u-ary amplitude and phase modulation (APM) scheme, a total of

$$m_F = \underbrace{\left\lfloor \log_2 \binom{L}{K_F} \right\rfloor}_{\text{Index bits}} + \underbrace{K_F \log_2 M_F}_{\text{Symbol bits}}, \qquad (1)$$

bits are conveyed by the FU signal per subblock. Similarly, in each subblock of the NU signal, total data bits are

$$m_N = \underbrace{\left\lfloor \log_2 \binom{K_F}{K_N} \right\rfloor}_{\text{Index bits}} + \underbrace{K_N \log_2 M_N}_{\text{Symbol bits}}. \qquad (2)$$

The vector of the modulated symbols at K_u active subcarriers for the user u is given by

$$\mathbf{s}_u = [s_u(1), ..., s_u(K_u)]^T, \qquad (3)$$

where $s_u(\gamma) \in \mathcal{S}_u$, $\gamma \in \{1, 2, ..., K_u\}$ and $\mathcal{S}_u$ is the complex signal constellation of size M_u.

For high spectral efficiency and additional flexibility, we introduce the *Envelope Former* module to the transmitter. In this module, the indices of the active subcarriers are selected for each user according to the mixed data bits of FU and NU. Specifically, in each subblock, data bits for NU are added behind FU in the bit mixer to form one data stream. As we have discussed, the length of the data stream to form the envelope is

$$m_{index} = \left\lfloor \log_2 \binom{L}{K_F} \right\rfloor + \left\lfloor \log_2 \binom{K_F}{K_N} \right\rfloor, \qquad (4)$$

bits. The subcarrier index selector utilizes the first $\left\lfloor \log_2 \binom{L}{K_F} \right\rfloor$ bits to decide the subcarrier activation pattern of the FU subblock, and the remaining bits are for the NU subblock. Then the OFDM subblock is produced by the subcarrier mapper, which can be expressed as follows

$$\mathbf{x}_u = [x_u(1), x_u(2), ..., x_u(L)]^T, \qquad (5)$$

where $x_u(\gamma) \in \{0, \mathcal{S}\}$ and $\gamma \in \{1, ..., L\}$. The indices set of the active subcarriers is given by

$$\mathbf{I}_u = \{I_u(1), I_u(2), ..., I_u(K_u)\}, \qquad (6)$$

where $I_u(1) < ... < I_u(K_u)$ and $I_u(k) \in \{1, 2, ..., L\}$. An example of the mapping table is presented in Table II for $L = 4$, $K_F = 3$, and $K_N = 2$.

Afterwards, G OFDM subblocks of user u are concatenated together to form one OFDM block before the power allocation. To distinguish signals of two users, different transmit power levels P_N and P_F are allocated to NU and FU, respectively, and $P_N + P_F = P_{\max}$. Since the channel gain for the NU is higher than the FU due to the distance difference, a higher power level is allocated to FU for user fairness, i.e $P_F > P_N$. We denote $P_u = a_u P_{max}$, where power allocation coefficients fulfill $a_N + a_F = 1$. In addition, we denote $\alpha_u = \sqrt{P_u}$. After the superposition coding, the tagged subblock can be expressed as

$$\mathbf{x} = \sum_u \alpha_u \mathbf{x}_u. \qquad (7)$$

Later, the inverse fast Fourier transform (IFFT) is applied to obtain the time domain OFDM block. A cyclic prefix (CP) of length Q is added at the beginning of the OFDM block, and then the signal is transmitted to the users.

B. Data Detection at Receivers with Decoding Scheme

Here the data detection procedures for both NOMA users are presented. At the receiver, the fast Fourier transform is

---

[2]It can be easily extended to N-user NOMA clusters ($N > 2$). We will illustrate the effectiveness of the assumption later in this paper.
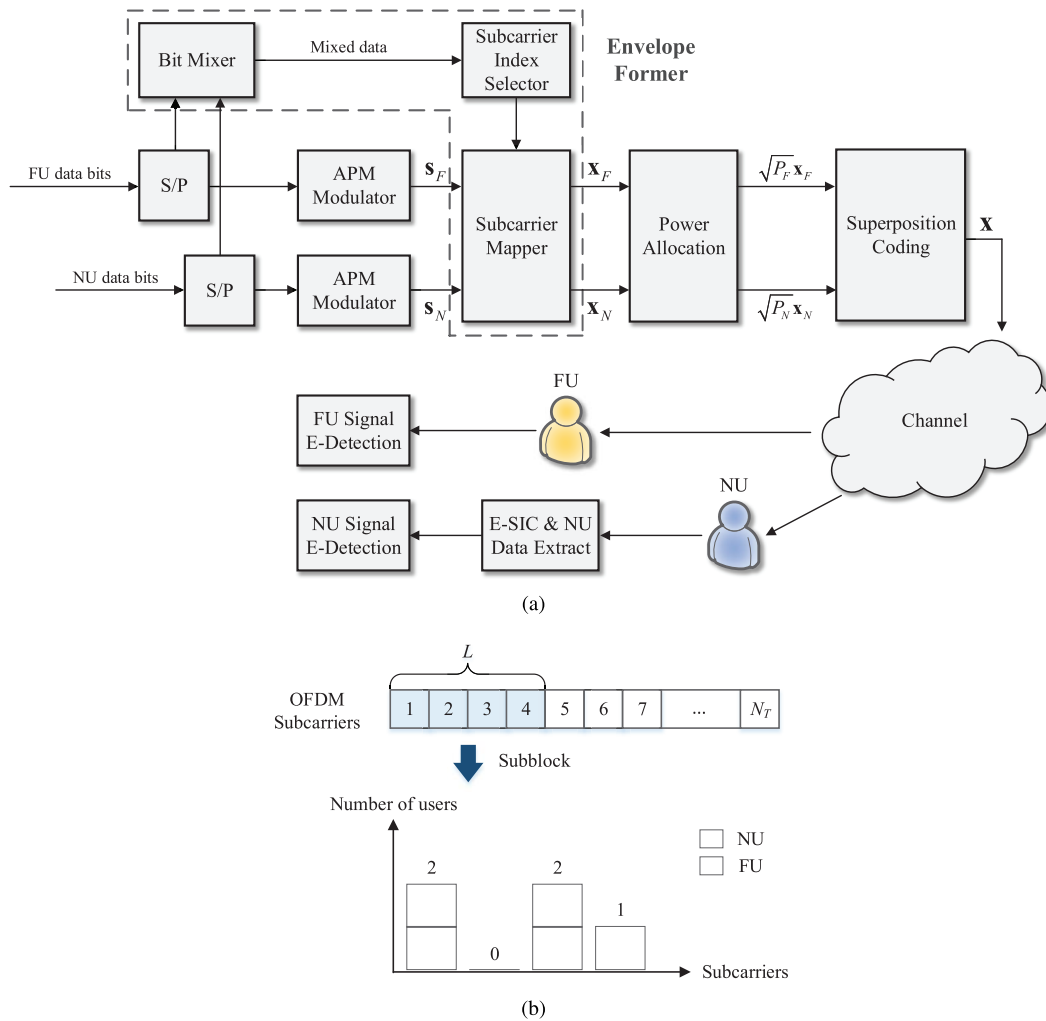
Fig. 1. Illustration of system model: (a) block diagram of the proposed NOMA-IE scheme; (b) a mapping example when $L = 4$, $K_F = 3$, $K_N = 2$, and mixed index bits are $[0, 1, 1]$.

TABLE II
AN EXAMPLE OF THE NOMA-IE MAPPING TABLE FOR $L = 4$, $K_F = 3$, AND $K_N = 2$

Mixed index bits	$\mathbf{I}_F$	FU subblock $\mathbf{x}_F$	$\mathbf{I}_N$	NU subblock $\mathbf{x}_N$
$[0, 0, 0]$	$\{2, 3, 4\}$	$[0, s_F(1), s_F(2), s_F(3)]^T$	$\{3, 4\}$	$[0, 0, s_N(1), s_N(2)]^T$
$[0, 0, 1]$	$\{2, 3, 4\}$	$[0, s_F(1), s_F(2), s_F(3)]^T$	$\{2, 3\}$	$[0, s_N(1), s_N(2), 0]^T$
$[0, 1, 0]$	$\{1, 3, 4\}$	$[s_F(1), 0, s_F(2), s_F(3)]^T$	$\{3, 4\}$	$[0, 0, s_N(1), s_N(2)]^T$
$[0, 1, 1]$	$\{1, 3, 4\}$	$[s_F(1), 0, s_F(2), s_F(3)]^T$	$\{1, 3\}$	$[s_N(1), 0, s_N(2), 0]^T$
$[1, 0, 0]$	$\{1, 2, 4\}$	$[s_F(1), s_F(2), 0, s_F(3)]^T$	$\{2, 4\}$	$[0, s_N(1), 0, s_N(2)]^T$
$[1, 0, 1]$	$\{1, 2, 4\}$	$[s_F(1), s_F(2), 0, s_F(3)]^T$	$\{1, 2\}$	$[s_N(1), s_N(2), 0, 0]^T$
$[1, 1, 0]$	$\{1, 2, 3\}$	$[s_F(1), s_F(2), s_F(3), 0]^T$	$\{2, 3\}$	$[0, s_N(1), s_N(2), 0]^T$
$[1, 1, 1]$	$\{1, 2, 3\}$	$[s_F(1), s_F(2), s_F(3), 0]^T$	$\{1, 2\}$	$[s_N(1), s_N(2), 0, 0]^T$

applied after removing the CP. The frequency domain signal vector received by the user u is expressed as follows

$$\mathbf{y}_u = \mathbf{X}\mathbf{h}_u + \mathbf{w}, \qquad (8)$$

where $\mathbf{h}_u = [h_u(1), h_u(2), ..., h_u(L)]^T$ and $\mathbf{w} = [w(1), w(2), ..., w(L)]^T$ denote the channel vector and the additive white Gaussian noise vector, respectively. For $\gamma \in \{1, 2, ..., L\}$, $w(\gamma) \sim \mathcal{CN}(0, N_0)$ and $h_u(\gamma) \sim \Omega_u \mathcal{CN}(0, 1)$, where Ω_u is the average channel gain. Usually, $\Omega_N > \Omega_F$ holds in NOMA systems.

The SIC process is employed as in conventional NOMA systems. Without loss of generality, we assume that the SIC is always processed at the NU. Therefore, the NU has to detect and subtract the FU signal before decoding its message. The SIC detection of conventional OFDM-NOMA in a subcarrier-by-subcarrier manner is not feasible here due to the envelope information conveyed by subblock realizations. Hence the NOMA-IE subblocks must be processed as a whole for detection. Therefore, we employ an envelope-detected SIC (E-SIC) in NOMA-IE. In the E-SIC process, the NU performs a joint

search for all possible combinations of the activation patterns and the constellation symbols according to the mapping table. The detected FU subblock can be given by

$$\hat{\mathbf{x}}_{F,SIC} = \arg\min_{\mathbf{x}_F \in \chi_F} \sum_{\gamma=1}^{L} \left| y_N(\gamma) - \beta_e \alpha_F \tilde{h}_N(\gamma) x_F(\gamma) \right|^2, \quad (9)$$

where $\beta_e > 0$ is the envelope detection coefficient. In the conventional SIC process, we have $\beta_e = 1$. χ_F stands for the possible realization set of the FU subblock $\mathbf{x}_F$. $\tilde{\mathbf{h}}_N = [\tilde{h}_N(1), \tilde{h}_N(2), ..., \tilde{h}_N(L)]^T$ is the estimated channel vector at the NU. Note that the index bits of the FU signal can be decoded by the NU, the NU can use at most m_{index} bits of index information without extra detection complexity.

After the E-SIC process, the subblock is given by $\mathbf{y}_{N,SIC} = \mathbf{y}_N - \alpha_F \hat{\mathbf{X}}_{F,SIC} \tilde{\mathbf{h}}_N$. By utilizing the knowledge of active subcarrier indices of the FU signal, i.e., $\hat{\mathbf{I}}_{F,SIC}$, the NU is able to detect both the index bits and the symbol bits from these indices by the envelope-detected detection (E-detection). Similar to the E-SIC, the E-detection procedure detects the data bits on the envelope and modulated constellations simultaneously. The detected NU subblock is

$$\hat{\mathbf{x}}_N = \arg\min_{\mathbf{x}_N \in \chi_N} \sum_{\gamma \in \hat{\mathbf{I}}_{F,SIC}} \left| y_{N,SIC}(\gamma) - \alpha_N \tilde{h}_N(\gamma) x_N(\gamma) \right|^2, \quad (10)$$

where χ_N represents the possible realization set of the NU subblock $\mathbf{x}_N$ conditioned on $\hat{\mathbf{I}}_{F,SIC}$.

Different from the NU, the FU decodes its message directly, treating the NU signal as interference. The FU subblock is detected by

$$\hat{\mathbf{x}}_F = \arg\min_{\mathbf{x}_F \in \chi_F} \sum_{\gamma=1}^{L} \left| y_F(\gamma) - \beta_e \alpha_F \tilde{h}_F(\gamma) x_F(\gamma) \right|^2, \quad (11)$$

where $\tilde{\mathbf{h}}_F = [\tilde{h}_F(1), \tilde{h}_F(2), ..., \tilde{h}_F(L)]^T$ is the estimated channel vector at the FU. It should be noted that an extra detection procedure is required if the FU uses the index information of the NU signal.

III. PRELIMINARY ANALYSIS

In this section, we analyze the spectral efficiency, energy efficiency, and detection complexity of the proposed NOMA-IE. The fundamental characteristics of NOMA-IE are revealed based on the three performance metrics. The performance of NOMA-IE is also compared with different OFDM-based schemes. Detailed discussions of the considered performance metrics are provided in the following subsections.

A. Spectral Efficiency

The spectral efficiency is defined as the ratio of the number of data bits in transmission to the total number of OFDM subcarriers in the considered OFDM block [16], which is given by

$$SE = \frac{N_t/L \times \sum_u m_u}{N_t + Q} \text{ bits/s/Hz}, \quad (12)$$

where $\sum_u m_u$ is the overall transmitted data bits in an OFDM subblock and $u \in \{N, F\}$.

Based on this definition, we obtain the spectral efficiency expressions in Table III straightforwardly. In those OMA schemes including conventional OFDM and OFDM-IM, we use K and M to represent the number of active subcarriers in each subblock and the order of APM, respectively. Since two users are grouped in NOMA schemes, paired users are considered in OMA schemes for a fair comparison. It is obvious that NOMA improves spectral efficiency. Moreover, by appropriately selecting K_u, IM-NOMA and NOMA-IE can achieve higher spectral efficiency performance than OFDM-NOMA.

B. Energy Efficiency

We regard the ratio of transmitted data bits to the total average energy consumption as energy efficiency. Here the CP is ignored for simplicity. Two transmit-power management policies are considered as follows.

1) Maximum Transmit Power Policy: The maximum power of each subcarrier is limited by P_{max}. The energy efficiency is expressed as

$$EE = \frac{\sum_u m_u}{P_{max} \sum_u a_u K_u} \text{ bits/J}. \quad (13)$$

2) Power Reallocation Policy: As in [30], the amplitude of each subcarrier is scaled by $\sqrt{\frac{L}{\sum_u a_u K_u}}$, and the energy efficiency is given by

$$EE = \frac{\sum_u m_u}{L P_{max}} \text{ bits/J}. \quad (14)$$

We compare the energy efficiency in the maximum transmit power policy of different OFDM-based schemes in Table III. In the power reallocation policy, the energy consumptions of all the considered schemes are equal, so we do not list this policy in the table. The NOMA-IE is highly energy-efficient in the maximum transmit power policy because the OFDM-IM framework enables the OFDM waveform to transmit more data bits by the same number of active subcarriers than the conventional OFDM.

C. Detection Complexity

We employ the optimal maximum-likelihood (ML) detector at receivers. To extract all information from the superposed signal, the detection complexity considers both the FU subblock and the NU subblock. In NOMA-IE, the FU subblock has $2^{\lfloor \log_2 \binom{L}{K_F} \rfloor} M_F^{K_F}$ different realizations, where $2^{\lfloor \log_2 \binom{L}{K_F} \rfloor}$ and $M_F^{K_F}$ are realization numbers of the subcarrier activation pattern and modulated symbol, respectively. Then the detection complexity per subcarrier in the FU subblock can be expressed as $\mathcal{O}\left(2^{\lfloor \log_2 \binom{L}{K_F} \rfloor} M_F^{K_F}/L\right)$. Similarly, the per subcarrier detection complexity is $\mathcal{O}\left(2^{\lfloor \log_2 \binom{K_F}{K_N} \rfloor} M_N^{K_N}/L\right)$ for the NU subblock. Detection complexity expressions of different schemes are summarized in Table III. It can be observed that the OFDM-IM framework brings high computational complexity to the ML detector. Therefore, high spectral and energy

efficiency can be achieved by NOMA-IE but high detection complexity is required at the same time[3].

IV. Error Probability Analysis

In this section, we focus on the error probabilities including the BLER and BER with the BPSK modulation. The perfect instantaneous CSI is assumed.

As we have stated, the detector of NOMA-IE treats the OFDM subblock as a whole rather than detects the signal subcarrier by subcarrier. Therefore, we introduce the BLER to characterize the error probability of the subblock of NOMA-IE. BLER is defined as the ratio of the number of subblocks in error to the total of OFDM subblocks. In NOMA-IE, there are two independent cases that lead to the erroneous subblock:

1) Index Error Existence (IEE) Case: Indices of active subcarriers are erroneous. In this case, the index bits are in error while the symbol bits have a probability to be correct.

2) Only Symbol Error (OSE) Case: Indices of active subcarriers are correctly detected, but symbol bits are erroneous.

For the user u subblock, let $P_{\text{IEE},u}$ and $P_{\text{OSE},u}$ denote the probabilities that the IEE case and OSE case occur, respectively. The BLER for the user u subblock can be expressed as

$$P_{l,u} = P_{\text{IEE},u} + P_{\text{OSE},u}. \tag{15}$$

BER is defined as the ratio of the number of data bits in error to the total of data bits transmitted by the OFDM subblock. We employ $m_{e1,g,u}$ and $m_{e2,g,u}$ to denote the number of error bits in subblock g for these two cases, respectively. Note that the index bits can be "borrowed from" or "lent to" the other NOMA user as we have discussed, error bits $\Delta m_{e1,g,u}$ and transmitted error bits Δm_u are considered. Thus, the BER for user u can be expressed as

$$P_{b,u} = \frac{\sum_g \left(m_{e1,g,u} + m_{e2,g,u} + \Delta m_{e1,g,u} \right)}{N_t/L \left(m_u + \Delta m_u \right)}. \tag{16}$$

A. Conditional Pairwise Error Probability

To characterize the error performance, we first focus on the error probability that the subblock is incorrectly detected. For FU subblock detection at FU, the error probability conditioned on known channel statement information (CSI) is expressed as

$$\Pr\left(\mathbf{x}_F \to \hat{\mathbf{x}}_F | \mathbf{h}_F\right) = \Pr\left(\bigcap_{\mathbf{z}_F \in \chi_F \setminus \hat{\mathbf{x}}_F} \left\{ \left\| \mathbf{y}_F - \beta_e \alpha_F \mathbf{Z}_F \mathbf{h}_F \right\|^2 \right. \right.$$
$$\left. \left. > \left\| \mathbf{y}_F - \beta_e \alpha_F \hat{\mathbf{X}}_F \mathbf{h}_F \right\|^2 \right\} \right). \tag{17}$$

The conditional error probabilities of the SIC process and NU subblock detection can be expressed similarly. However, it is difficult to calculate the exact probability when the number of possible realizations in χ_u is larger than two. As in most existing works, we utilize the pairwise error probability (PEP) as an approximation to simplify our derivations [31].

---

[3]Low-complexity sub-optimal detection methods will be investigated in our future work.

Approximation 1. *PEPs are the tight upper bounds of error probabilities in FU subblock detection, SIC process, and NU subblock detection. The conditional PEP expressions are given by*

$$\Pr\left(\mathbf{X}_F \to \hat{\mathbf{X}}_F | \mathbf{h}_F\right) \approx \Pr\left(\left\| \mathbf{y}_F - \beta_e \alpha_F \mathbf{X}_F \mathbf{h}_F \right\|^2 \right.$$
$$\left. > \left\| \mathbf{y}_F - \beta_e \alpha_F \hat{\mathbf{X}}_F \mathbf{h}_F \right\|^2 \right), \tag{18}$$

$$\Pr\left(\mathbf{X}_F \to \hat{\mathbf{X}}_F | \mathbf{h}_N\right) \approx \Pr\left(\left\| \mathbf{y}_N - \beta_e \alpha_F \mathbf{X}_F \mathbf{h}_N \right\|^2 \right.$$
$$\left. > \left\| \mathbf{y}_N - \beta_e \alpha_F \hat{\mathbf{X}}_F \mathbf{h}_N \right\|^2 \right), \tag{19}$$

$$\Pr\left(\mathbf{X}_N \to \hat{\mathbf{X}}_N | \mathbf{h}_N\right) \approx \Pr\left(\left\| \mathbf{y}_{N,SIC} - \alpha_N \mathbf{X}_N \mathbf{h}_N \right\|^2 \right.$$
$$\left. > \left\| \mathbf{y}_{N,SIC} - \alpha_N \hat{\mathbf{X}}_N \mathbf{h}_N \right\|^2 \right), \tag{20}$$

which converge to exact results at high SNR. Moreover, these approximations become exact when the subblock only has one OFDM symbol with the binary modulation.

Before the analysis of NOMA-IE, we provide some simple conditional PEP expressions in both the conventional OFDM and the OFDM-IM framework, which are helpful to derive expressions in the NOMA-IE. In conventional OFDM, symbols can be detected separately, so we focus on one OFDM subcarrier. Noticing that NOMA-IE can be regarded as a mixture of NOMA and OMA schemes, here we consider both the OMA and NOMA cases. Since the FU detects the superimposed signal directly, we denote the amplitude of the superimposed symbol as $|x(\gamma)| \triangleq \lambda_F \in \mathbf{\Lambda} = \{\lambda_-, \lambda_*, \lambda_+\}$ and the elements in $\mathbf{\Lambda}$ are given by

$$\lambda_- = \alpha_F - \alpha_N, \tag{21a}$$
$$\lambda_* = \alpha_F, \tag{21b}$$
$$\lambda_+ = \alpha_F + \alpha_N. \tag{21c}$$

After the SIC process, the signal for the NU is OMA, and the amplitude of the NU symbol is $\alpha_N \triangleq \lambda_N$. Then the conditional PEP is expressed as follows.

Proposition 1. *In conventional OFDM, the conditional PEP for user u is given by [25]*

$$P_{C,u}(\lambda_u, \mathbf{h}_u) = Q\left(\sqrt{\frac{2 \left\| \lambda_u \mathbf{h}_u \right\|^2}{N_0}} \right). \tag{22}$$

In the OFDM-IM framework, we consider a simple two-subcarrier subblock where only one subcarrier is active. According to **Assumption 1**, all the possible realizations of a superimposed subblock are $\chi = \{[\lambda_F, 0]^T, [-\lambda_F, 0]^T, [0, \lambda_F]^T, [0, -\lambda_F]^T\}$. We assume $\mathbf{x} = [\lambda_F, 0]^T$ due to the symmetry of modulation constellations. As we have discussed, two categories of error exist in the OFDM-IM. Therefore, there are two cases for the PEP expression.

TABLE III
PERFORMANCE COMPARISONS OF DIFFERENT OFDM-BASED SCHEMES

Scheme	Spectral efficiency	Energy efficiency	Detection complexity
Conventional OFDM	$\frac{N_T \log_2 M}{N_T+Q}$	$\frac{\log_2 M}{P_{max}}$	$\mathcal{O}(M)$
OFDM-NOMA [29]	$\frac{N_T \sum_u \log_2 M_u}{N_T+Q}$	$\frac{\sum_u \log_2 M_u}{P_{max}}$	$\mathcal{O}\left(\sum_u M_u\right)$
OFDM-IM [12]	$\frac{N_T\left(\left\lfloor\log_2\binom{L}{K}\right\rfloor+K\log_2 M\right)}{L(N_T+Q)}$	$\frac{\left\lfloor\log_2\binom{L}{K}\right\rfloor+K\log_2 M}{KP_{max}}$	$\mathcal{O}\left(\frac{2^{\left\lfloor\log_2\binom{L}{K}\right\rfloor}M^K}{L}\right)$
IM-NOMA [20]	$\frac{N_T\sum_u\left(\left\lfloor\log_2\binom{L}{K_u}\right\rfloor+K_u\log_2 M_u\right)}{L(N_T+Q)}$	$\frac{\sum_u\left(\left\lfloor\log_2\binom{L}{K_u}\right\rfloor+K_u\log_2 M_u\right)}{P_{max}\sum_u a_u K_u}$	$\mathcal{O}\left(\sum_u\frac{2^{\left\lfloor\log_2\binom{L}{K_u}\right\rfloor}M^{K_u}}{L}\right)$
NOMA-IE (this paper)	$\frac{N_T\left(\left\lfloor\log_2\binom{L}{K_F}\right\rfloor+K_F\log_2 M_F\right)}{L(N_T+Q)}+$ $\frac{N_T\left(\left\lfloor\log_2\binom{K_F}{K_N}\right\rfloor+K_N\log_2 M_N\right)}{L(N_T+Q)}$	$\frac{\left\lfloor\log_2\binom{L}{K_F}\right\rfloor+K_F\log_2 M_F}{P_{max}\sum_u a_u K_u}+$ $\frac{\left\lfloor\log_2\binom{K_F}{K_N}\right\rfloor+K_N\log_2 M_N}{P_{max}\sum_u a_u K_u}$	$\mathcal{O}\left(2^{\left\lfloor\log_2\binom{L}{K_F}\right\rfloor}M_F^{K_F}/L\right)+$ $\mathcal{O}\left(2^{\left\lfloor\log_2\binom{K_F}{K_N}\right\rfloor}M_N^{K_N}/L\right)$

Proposition 2. *In the OFDM-IM framework, if the index information is erroneously detected, i.e., the IEE case occurs, the conditional PEPs for the FU and NU are separately given by*

$$P_{I,F}(\lambda_F, \mathbf{h}_F)$$
$$= Q\left(\frac{\left(\lambda_F - \frac{1}{2}\beta_e\lambda_*\right)\|h_F(1)\|^2 + \frac{1}{2}\beta_e\lambda_*\|h_F(2)\|^2}{\sqrt{\frac{N_0}{2}\left(\|h_F(1)\|^2 + \|h_F(2)\|^2\right)}}\right),$$
$$(23)$$

$$P_{I,N}(\lambda_N, \mathbf{h}_N) = Q\left(\sqrt{\frac{\|\lambda_N h_N(1)\|^2 + \|\lambda_N h_N(2)\|^2}{2N_0}}\right).$$
$$(24)$$

If the subblock only has an incorrect symbol, i.e., the OSE case occurs, the conditional PEP for user u can be expressed as

$$P_{S,u}(\lambda_u, \mathbf{h}_u) = Q\left(\sqrt{\frac{2\|\lambda_u h_u(1)\|^2}{N_0}}\right). \qquad (25)$$

Moreover, for the SIC process, we have $P_{I,SIC}(\lambda_F, \mathbf{h}_N) = P_{I,F}(\lambda_F, \mathbf{h}_N)$ and $P_{S,SIC}(\lambda_F, \mathbf{h}_N) = P_{S,F}(\lambda_F, \mathbf{h}_N)$.

Proof: The received superposed subblock at FU is $\mathbf{y}_F = [h_F(1)\lambda_F + w(1), w(2)]^T$. The ML detector compares $\mathbf{y}_F$ with each element in set $\left\{\pm[h_F(1)\beta_e\lambda_*, 0]^T, \pm[0, h_F(2)\beta_e\lambda_*]^T\right\}$ and finds the closest element. We denote $\mathbf{z}_F = [h_F(1)\beta_e\lambda_*, 0]^T$ and $\hat{\mathbf{z}}_F = [0, h_F(2)\beta_e\lambda_*]^T$. In the IEE case, the conditional PEP of FU is calculated as

$$P_{I,F}(\lambda_F, \mathbf{h}_F) = \Pr\left(\|\mathbf{y}_F - \mathbf{z}_F\|^2 > \|\mathbf{y}_F \pm \hat{\mathbf{z}}_F\|^2\right)$$
$$= \Pr\left(\delta > \left(\lambda_F - \frac{\beta_e\lambda_*}{2}\right)\|h_F(1)\|^2 \right.$$
$$\left. + \frac{\beta_e\lambda_*}{2}\|h_F(2)\|^2\right), \quad (26)$$

where $\delta = h_F(1)w(1) \pm h_F(2)w(2)$ is a Gaussian random variable with mean 0 and variance $\sigma^2 = \frac{N_0\left(\|h_F(1)\|^2 + \|h_F(2)\|^2\right)}{2}$.

Utilizing the property of Gaussian random variable that $\Pr(\delta > x) = Q\left(\frac{x}{\sigma}\right)$, (23) is proved. Using similar proof, other conditional PEP expressions in this proposition can be obtained. ∎

It can be observed from (25) that under OFDM-IM, the PEP expression of the OSE case is the same as that in the conventional OFDM system. In this case, the error performance is unrelated to the channel condition of the inactive subcarrier and the envelope detection coefficient. However, if the IEE case occurs, the error performance in the NOMA setup shown in (23) is much different from the conventional counterpart. In the following lemma, we illustrate cases where the intra-cluster interference in NOMA causes the error floor.

Lemma 1. *The detection error floor exists when $\alpha_F \leq \frac{2\alpha_N}{2-\beta_e}$.*

Proof: If the detection error floor exists, the conditional PEP is not zero when the transmit SNR $P_{max}/N_0 \to \infty$. According to the property of the Q-function, when $x \to +\infty$ we have $Q(x) \to 0$. It can be observed from (23) that $\lambda_F - \frac{1}{2}\beta_e\lambda_* > 0$ guarantees the conditional PEP is 0 when SNR becomes large. Then the proof is completed. ∎

Corollary 1. *If the envelope detection coefficient $\beta_e = 1$, the error floor always exists when $\alpha_F \leq 2\alpha_N$. That is to say, the feasible range of power allocation coefficients for the paired NOMA-IE users is $P_F > 4P_N$.*

Corollary 2. *If the envelope detection coefficient $\beta_e = \frac{\alpha_F - \alpha_N}{\alpha_F}$, $\alpha_F > \frac{2\alpha_N}{2-\beta_e}$ always holds. In this case, the error floor is eliminated. We denote*

$$\beta_0 = \frac{\alpha_F - \alpha_N}{\alpha_F} = \frac{\sqrt{a_F} - \sqrt{a_N}}{\sqrt{a_F}}, \qquad (27)$$

as the feasible envelope detection coefficient.

To understand the reason that results in the error floor more easily, we illustrate the construction of the superimposed symbols for the case $\alpha_F = 2\alpha_N$ in Fig. 2, where the constellations with normalized energy are considered, i.e., $d_u = \frac{\alpha_u}{\sqrt{P_{max}}}$ for $u \in \{F, N\}$. It is observed that some superimposed constellation points cannot be distinguished in IM-NOMA when $\alpha_F \leq 2\alpha_N$, which leads to the error floor no matter what value β_e is. Different from the IM-NOMA, the
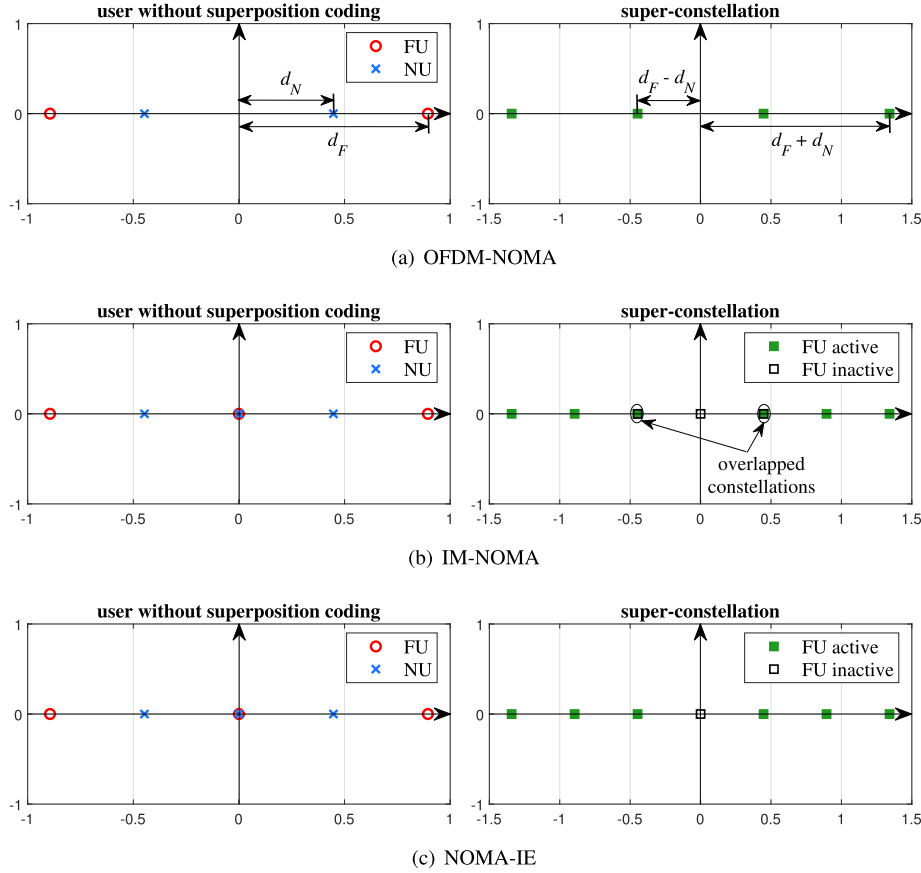
Fig. 2. The construction of the superimposed symbols with $\alpha_F = 2\alpha_N$.

design of NOMA-IE (**Assumption 1**) avoids the constellation overlap, and hence the appropriate β_e helps to eliminate the error floor.

Remark 2. *In NOMA-IE, the feasible range of power allocation coefficients for the paired NOMA-IE users is the same as that in conventional NOMA systems, i.e., $a_F > a_N$.*

By leveraging these conditional PEP expressions in the conventional OFDM and OFDM-IM frameworks, the theoretical BLER and BER for the NOMA-IE can be calculated based on the concept of TSE, which is discussed in the following subsection.

B. Two-Subcarrier Element

In this work, we introduce the concept of TSE for ease of calculation. TSE is defined as a two-subcarrier superposed subblock, where $K_F = K_N = 1$. Therefore, for each TSE, the FU subblock conveys one bit symbol bits and one bit index bits, while the NU subblock only conveys one bit symbol bits.

The TSE can be regarded as the simplest NOMA-IE subblock in which part of data bits can be conveyed by the envelope. Here we derive the BLER and BER of the TSE as priliminary. If all the constellation points are equiprobable, the average BLER of the detected FU subblock at the FU can be expressed as

$$P_{l,F} = \frac{1}{\xi_F \xi_N} \sum_{\mathbf{x}_F} \sum_{\mathbf{x}_N} \sum_{\hat{\mathbf{x}}_F \neq \mathbf{x}_F} \Pr\left(\mathbf{x}_F \to \hat{\mathbf{x}}_F | \mathbf{x}_N\right), \quad (28)$$

where ξ_F and ξ_N are the numbers of possible realizations for the FU subblock and the NU subblock, respectively. Utilizing the symmetry of constellations, we assume that $\mathbf{x}_F = [1, 0]^T$, and (28) can be rewritten as

$$P_{l,F} = \frac{1}{2} \sum_{\lambda_F \in \{\lambda_-, \lambda_+\}} \left(P_{S,F}(\lambda_F) + 2P_{I,F}(\lambda_F)\right), \quad (29)$$

where $P_{S,F}(\lambda)$ and $P_{I,F}(\lambda)$ are the unconditional PEPs obtained from **Proposition 2**. Adopting $Q(x) \cong \frac{1}{12}e^{-x^2/2} + \frac{1}{4}e^{-2x^2/3}$ as the approximation of the Q-function [32], $P_{S,F}(\lambda)$ is given by

$$
\begin{aligned}
P_{S,F}(\lambda) &= \int_{\mathbf{h}_F} Q\left(\lambda\sqrt{\frac{2\|\mathbf{h}_F\|^2}{N_0}}\right) f(\mathbf{h}_F)\, d\mathbf{h}_F \\
&\cong \mathbb{E}_{\|\mathbf{h}_F\|^2}\left(\frac{1}{12}e^{-\frac{\lambda^2\|\mathbf{h}_F\|^2}{N_0}} + \frac{1}{4}e^{-\frac{4\lambda^2\|\mathbf{h}_F\|^2}{3N_0}}\right) \\
&= \frac{1/12}{\Omega_F \lambda^2/N_0 + 1} + \frac{1/4}{4\Omega_F \lambda^2/3N_0 + 1}.
\end{aligned}
\quad (30)
$$

The unconditional PEP $P_{I,F}(\lambda)$ is expressed as

$$
P_{I,F}(\lambda) = \int_0^\infty \int_0^\infty Q\left(\Omega_F \frac{\left(\lambda - \frac{1}{2}\beta_e\lambda_*\right)h_1 + \frac{1}{2}\beta_e\lambda_* h_2}{\sqrt{\frac{N_0}{2}(h_1 + h_2)}}\right) \\
\times f(h_1)f(h_2)dh_1 dh_2,
\quad (31)
$$

where $f(x) = \exp(-x)$ due to the Rayleigh fading. When $a_F \to 1$, the interference from the NU is negligible, and hence the $P_{I,F}(\lambda)$ can be further simplified as

$$P_{I,F}(\lambda_F) \cong P_{I,F}(\lambda_*)$$
$$= \frac{1/12}{\det\left(q_1 \Omega_F \mathbf{A} + \mathbf{I}_2\right)} + \frac{1/4}{\det\left(q_2 \Omega_F \mathbf{A} + \mathbf{I}_2\right)}, \quad (32)$$

where $\mathbf{A}_F = (\mathbf{X}_F - \hat{\mathbf{X}}_F)^H (\mathbf{X}_F - \hat{\mathbf{X}}_F)$, $q_1 = \frac{1}{4N_0}$, and $q_2 = \frac{1}{3N_0}$.

We use $e(\mathbf{x}, \hat{\mathbf{x}})$ to denote the number of error bits when $\mathbf{x}$ is erroneously detected as $\hat{\mathbf{x}}$. The average BER of the detected FU subblock at the FU can be calculated as follows

$$P_{b,F} = \frac{1}{m_F \xi_F \xi_N} \sum_{\mathbf{x}_F} \sum_{\mathbf{x}_N} \sum_{\hat{\mathbf{x}}_F \neq \mathbf{x}_F} \Pr\left(\mathbf{x}_F \to \hat{\mathbf{x}}_F | \mathbf{x}_N\right) e\left(\mathbf{x}_F, \hat{\mathbf{x}}_F\right)$$
$$= \frac{1}{2m_F} \sum_{\lambda_F \in \{\lambda_-, \lambda_+\}} \left(P_{S,F}(\lambda_F) + 3P_{I,F}(\lambda_F)\right). \quad (33)$$

Since the length of the NU subblock is $K_N = 1$, the BLER of NU is equal to BER with the BPSK modulation. For the NU, the E-SIC process occurs first. The probability of the imperfect E-SIC conditioned on the known $\mathbf{x}_N$ can be expressed as

$$P_{e,SIC|\mathbf{x}_N} = \sum_{\hat{\mathbf{x}}_{F,SIC} \neq \mathbf{x}_{F,SIC}} \Pr\left(\mathbf{x}_{F,SIC} \to \hat{\mathbf{x}}_{F,SIC} | \mathbf{x}_N\right). \quad (34)$$

The calculation of (34) is the same as $P_{l,F}$. When the FU subblock is detected incorrectly, the situation for the re-constructed signal $\mathbf{y}_{N,SIC}$ is complex. Part of NOMA interference improves the amplitudes of symbols, while the other part of interference degrades the error performance. For simplicity, we make an approximation to calculate the BER of the NU under imperfect E-SIC.

Approximation 2. *Considering BPSK, the BER of the NU is 0.5 when the error occurs during the E-SIC process. This approximation is based on the assumption that all the constellation points of the FU and the NU are equiprobable.*

This approximation is accurate when $a_F \to 1$. Then the average BLER and BER of the NU subblock can be approximated by

$$P_{l,N} = P_{b,N}$$
$$\approx \frac{1}{\xi_N} \sum_{\mathbf{x}_N} \left\{ \frac{1}{2} P_{e,SIC|\mathbf{x}_N} + \frac{1 - P_{e,SIC|\mathbf{x}_N}}{m_N} \right.$$
$$\left. \times \sum_{\hat{\mathbf{x}}_N \neq \mathbf{x}_N} \Pr\left(\mathbf{x}_N \to \hat{\mathbf{x}}_N\right) e\left(\mathbf{x}_N, \hat{\mathbf{x}}_N\right) \right\}$$
$$= \frac{1}{2} P_{e,SIC} + \frac{1}{2} \sum_{\mathbf{x}_N} \left\{ \left(1 - P_{e,SIC|\mathbf{x}_N}\right) P_{C,N}(\lambda_N) \right\}, \quad (35)$$

where the calculation of $P_{C,N}(\lambda)$ is similar to (30)

$$P_{C,N}(\lambda) \cong \frac{1/12}{\Omega_N \lambda^2 / N_0 + 1} + \frac{1/4}{4\Omega_N \lambda^2 / 3N_0 + 1}. \quad (36)$$

From (35) we observe that the probability of the imperfect E-SIC $P_{e,SIC|\mathbf{x}_N}$ is a significant component of $P_{b,N}$ and $P_{l,N}$.

Therefore, a large $P_{e,SIC|\mathbf{x}_N}$ leads to poor error performance for the NU.

Remark 3. *A low BLER/BER of the NU in NOMA-IE heavily relies on the perfect E-SIC process. This conclusion can be extended to the general NOMA transmissions with the SIC process.*

C. Error Performance in Four-Subcarrier Subblocks

In this subsection, we consider $K_F = 3$ and $K_N = 2$ shown in Table II as an example. Similarly, we first focus on the FU. Based on **Approximation 1**, the unconditional PEP of the FU subblock

$$\Pr\left(\mathbf{x}_F \to \hat{\mathbf{x}}_F\right) = \int_{\tilde{\mathbf{h}}_F} \Pr\left(\left\| \mathbf{y}_F - \beta_e \alpha_F \mathbf{x}_F \tilde{\mathbf{h}}_F \right\|^2 \right.$$
$$\left. > \left\| \mathbf{y}_F - \beta_e \alpha_F \hat{\mathbf{x}}_F \tilde{\mathbf{h}}_F \right\|^2 \right) d\tilde{\mathbf{h}}_F, \quad (37)$$

has at least quadruple integral. The expression seems tedious and intractable.

Fortunately, the four-subcarrier superimposed subblock can be regarded as the combination of multiple TSEs. In particular, the superimposed subblock consists of K_F TSEs, and all these elements share the same inactive subcarrier. The number of active subcarriers in TSEs is one. Accordingly, we denote the kth TSE as $T_{F,k} = \{c_F(k), 0\}$ as the FU message is always detected first. The amplitude vector of symbols on active subcarriers is denoted by $\mathbf{c}_F = [c_F(1), ..., c_F(K_F)]^T \in \mathbb{C}^{K_F \times 1}$, where $c_F(k) \in \{\lambda_-, \lambda_*, \lambda_+\}$. Based on **Assumption 1**, $c_F(k)$ is equal to the amplitude of $x_F(I_F(k))$, i.e., $c_F(k) = |x_F(I_F(k))|$.

If the FU subblock can be detected correctly, no error occurs in any TSEs. Otherwise, at least one erroneous TSE leads to an incorrect FU subblock. Therefore, the average BLER of FU can be expressed as

$$P_{l,F} = 1 - \int_0^\infty \exp(-x)$$
$$\times \prod_{k=1}^{K_F} \left(1 - 2P_{I,F}(c_F(k), x) - P_{S,F}(c_F(k))\right) dx, \quad (38)$$

where

$$P_{I,F}(\lambda, x) = \int_0^\infty Q\left(\Omega_F \frac{\left(\lambda - \frac{1}{2}\beta_e \lambda_*\right) h_1 + \frac{1}{2}\beta_e \lambda_* x}{\sqrt{\frac{N_0}{2}(h_1 + x)}} \right)$$
$$\times f(h_1) dh_1. \quad (39)$$

To obtain the BER of FU, we calculate the number of error bits in the two independent error cases as follows.

1) IEE Case: In this case, the inactive subcarrier is erroneously detected as an active one. Therefore, the index error occurs in no less than one TSE. Since the probability that more than one TSE has the index error is ignorable at a high SNR, we employ the following approximation.

Approximation 3. *The number of incorrect inactive indices is equal to the number of TSEs with the index error. This approximation converges to the exact value when $\text{SNR} \to \infty$.*

For clarity, we first investigate the index error probability. We define $\hat{\mathbf{I}}_F(k)$ as the indices set of active subcarriers when kth TSE has the index error. The probability of erroneously detecting $\mathbf{I}_F$ as $\hat{\mathbf{I}}_F(k)$ can be calculated by

$$\Pr\left(\mathbf{I}_F \rightarrow \hat{\mathbf{I}}_F(k)\right) = \int_0^\infty 2P_{I,F}(c_F(k), x)\exp(-x)$$
$$\times \prod_{j=1, j\neq k}^{K_F} (1 - 2P_{I,F}(c_F(j), x))\,dx. \quad (40)$$

According to the law of total probability, the probability that $\mathbf{s}_F$ is erroneously detected by $\hat{\mathbf{s}}_F$ can be expressed as

$$\Pr\left(\mathbf{s}_F \rightarrow \hat{\mathbf{s}}_F | \hat{\mathbf{I}}_F \neq \mathbf{I}_F\right) = \sum_{k=1}^{K_F} \Pr\left(\mathbf{s}_F \rightarrow \hat{\mathbf{s}}_F | \mathbf{I}_F \rightarrow \hat{\mathbf{I}}_F(k)\right)$$
$$\times \Pr\left(\mathbf{I}_F \rightarrow \hat{\mathbf{I}}_F(k)\right), \quad (41)$$

where $\Pr\left(\mathbf{s}_F \rightarrow \hat{\mathbf{s}}_F | \mathbf{I}_F \rightarrow \hat{\mathbf{I}}_F(k)\right)$ represents the conditional PEP of detecting $\mathbf{s}_F$ as $\hat{\mathbf{s}}_F$ conditioned on $\mathbf{I}_F \rightarrow \hat{\mathbf{I}}_F(k)$. In the OFDM-IM framework, erroneous indices result in symbol unsynchronization. For example, if the FU subblock $\mathbf{x}_F = [s_F(1), s_F(2), s_F(3), 0]^T$ is incorrectly detected as $\hat{\mathbf{x}}_F = [\hat{s}_F(1), 0, \hat{s}_F(2), \hat{s}_F(3)]^T$, only $\hat{s}_F(1)$ is detected from $s_F(1)$. $\hat{s}_F(2)$ is detected from $s_F(2)$ and $\hat{s}_F(3)$ is from the noise. We denote $\mathbf{\Psi}_{\mathbf{I}_F \rightarrow \hat{\mathbf{I}}_F(k)}$ and $\bar{\mathbf{\Psi}}_{\mathbf{I}_F \rightarrow \hat{\mathbf{I}}_F(k)}$ as the synchronized symbol set and the unsynchronized symbol set conditioned on $\mathbf{I}_F \rightarrow \hat{\mathbf{I}}_F$, respectively, and we have $\mathbf{\Psi}_{\mathbf{I}_F \rightarrow \hat{\mathbf{I}}_F(k)} \bigcup \bar{\mathbf{\Psi}}_{\mathbf{I}_F \rightarrow \hat{\mathbf{I}}_F(k)} = \mathbf{I}_F$. The unsynchronized symbols can be detected as random constellation points of the employed modulation scheme. For those synchronized symbols, their error performance is related to channel conditions. We use $\mathbf{\Psi}_c$ and $\mathbf{\Psi}_e$ to denote the correct synchronized symbol set and the erroneous synchronized symbol set, respectively. Then the conditional PEP is given by

$$\Pr\left(\mathbf{s}_F \rightarrow \hat{\mathbf{s}}_F | \mathbf{I}_F \rightarrow \hat{\mathbf{I}}_F(k)\right) = 0.5^{|\bar{\mathbf{\Psi}}_{\mathbf{I}_F \rightarrow \hat{\mathbf{I}}_F(k)}|}$$
$$\times \prod_{I_F(i) \in \mathbf{\Psi}_c} P_{S,F}(c_F(i))$$
$$\times \prod_{I_F(j) \in \mathbf{\Psi}_e} P_{S,F}(1 - c_F(j)). \quad (42)$$

When the indices of the active subcarriers are erroneous, some symbols are detected from the random noise or unsynchronized symbols. Therefore, BER in the IEE case is much higher than in the case no index error occurs. How reduce the index error is an important issue for error performance improvement in the NOMA-IE.

Remark 4. *In the OFDM-IM framework, the index error is strongly correlated with the symbol error, and the high probability of the index error leads to significant performance degradation in BER.*

Afterwards, the number of error bits for the FU subblock

in the index error case can be calculated as

$$m_{e1,F} = \sum_{\hat{\mathbf{s}}_F \neq \mathbf{s}_F} \Pr\left(\mathbf{s}_F \rightarrow \hat{\mathbf{s}}_F | \hat{\mathbf{I}}_F \neq \mathbf{I}_F\right) e\left(\mathbf{s}_F \rightarrow \hat{\mathbf{s}}_F\right)$$
$$+ \sum_{\hat{\mathbf{I}}_F \neq \mathbf{I}_F} \Pr\left(\mathbf{I}_F \rightarrow \hat{\mathbf{I}}_F(k)\right) e\left(\mathbf{I}_F \rightarrow \hat{\mathbf{I}}_F(k)\right), \quad (43)$$

where $e\left(\mathbf{s}_F \rightarrow \hat{\mathbf{s}}_F\right)$ is the number of error bits when $\mathbf{s}_F$ is erroneously detected as $\hat{\mathbf{s}}_F$. $e\left(\mathbf{I}_F \rightarrow \hat{\mathbf{I}}_F(k)\right)$ is the number of error bits when $\mathbf{I}_F$ is erroneously detected as $\hat{\mathbf{I}}_F(k)$.

2) OSE Case: In this case, the index information is correct, the probability of which can be calculated as

$$P_{I,c} = 1 - \int_0^\infty \exp(-x) \prod_{k=1}^{K_F} (1 - 2P_{I,F}(c_F(k), x))\,dx. \quad (44)$$

Since the indices of the active subcarrier are correct, all symbols in the FU subblock are synchronized. The PEP conditioned on the correct index information can be expressed as

$$\Pr\left(\mathbf{s}_F \rightarrow \hat{\mathbf{s}}_F | \hat{\mathbf{I}}_F = \mathbf{I}_F\right) = \prod_{I_F(i) \in \mathbf{\Psi}_c} P_{S,F}(c_F(i))$$
$$\times \prod_{I_F(j) \in \mathbf{\Psi}_e} P_{S,F}(1 - c_F(j)). \quad (45)$$

Then the number of error bits for the FU subblock in the no index error case is given by

$$m_{e2,F} = P_{I,c} \sum_{\hat{\mathbf{s}}_F \neq \mathbf{s}_F} \Pr\left(\mathbf{s}_F \rightarrow \hat{\mathbf{s}}_F | \hat{\mathbf{I}}_F = \mathbf{I}_F\right) e\left(\mathbf{s}_F \rightarrow \hat{\mathbf{s}}_F\right). \quad (46)$$

As mentioned, no extra detection complexity is required if Δm_N out of $\left\lfloor \log_2\binom{L}{K_F} \right\rfloor$ bits index information of the FU subblock is used by the NU. When the NU utilizes the envelope of the FU subblock, the overall BER of the FU is

$$P_{b,F} = \frac{m_{e1,F} + m_{e2,F} + \Delta m_{e1,F}}{m_F - \Delta m_N}, \quad (47)$$

where

$$\Delta m_{e1,F} = -p_1 \sum_{\hat{\mathbf{I}}_F \neq \mathbf{I}_F} \Pr\left(\mathbf{I}_F \rightarrow \hat{\mathbf{I}}_F(k)\right) e\left(\mathbf{I}_F \rightarrow \hat{\mathbf{I}}_F(k)\right), \quad (48)$$

and $p_1 = \Delta m_N / \left\lfloor \log_2\binom{L}{K_F} \right\rfloor$.

At the NU, the E-SIC process is operated first. The probability of the imperfect E-SIC can be calculated as follows

$$P_{e,SIC} = \int_0^\infty \exp(-x)$$
$$\times \prod_{k=1}^{K_F} (2P_{I,SIC}(c_F(k), x) + P_{S,SIC}(c_F(k)))\,dx, \quad (49)$$

where

$$P_{I,SIC}(\lambda, x) = \int_0^\infty Q\left(\Omega_N \frac{\left(\lambda - \frac{1}{2}\beta_e\lambda_*\right)h_1 + \frac{1}{2}\beta_e\lambda_* x}{\sqrt{\frac{N_0}{2}(h_1 + x)}}\right)$$
$$\times f(h_1)dh_1. \quad (50)$$

The NU subblock consists of K_N TSEs. When $K_F = 3$ and $K_N = 2$, the NU subblock only conveys one-bit index bits. Conditioned on the perfect SIC, the IEE case occurs due to the error in specific TSE, and hence the probability of the IEE case is given by $P_{I,N,e} = 2P_{I,N}(\alpha_N)$. In this case, the subblock is correct with the probability $(1 - P_{S,N}(\alpha_N))^{K_N}(1 - P_{I,N,e})$. Conditioned on the imperfect SIC, the probability of the correct subblock is approximated as 0.5^{m_N} based on **Approximation 2**. Therefore, the average BLER of the NU subblock is

$$P_{l,N} \approx 1 - 0.5^{m_N}P_{e,SIC} - (1 - P_{S,N}(\alpha_N))^{K_N}$$
$$\times (1 - P_{I,N,e})(1 - P_{e,SIC}). \quad (51)$$

Conditioned on the perfect E-SIC, the calculation of the number of error bits for the NU subblock is similar to that of the FU subblock. The number of error bits for the IEE case and the OSE case of the NU subblock are separately given by

$$m_{e1,N} = \sum_{\hat{s}_N \neq s_N} 0.5^{K_N} e(s_N \to \hat{s}_N) + P_{I,N,e}, \quad (52)$$

$$m_{e2,N} = (1 - P_{I,N,e}) \sum_{i=1}^{K_N} i\left(P_{S,N}(\alpha_N)\right)^{K_N - i}$$
$$\times (1 - P_{S,N}(\alpha_N))^i. \quad (53)$$

If the E-SIC is imperfect, we adopt the approximation of the average BER as in the two-subcarrier subblock. The overall BER of the NU is approximated as

$$P_{b,N} \approx \frac{0.5 m_N P_{e,SIC} + (1 - P_{e,SIC})m_{e,N} + \Delta m_{e1,N}}{m_N + \Delta m_N}, \quad (54)$$

where $m_{e,N} = m_{e1,N} + m_{e2,N}$. $\Delta m_{e1,N}$ is the number of error bits from the FU envelope under imperfect SIC. The calculation of $\Delta m_{e1,N}$ is similar to $\Delta m_{e1,F}$, and hence we skip it here.

V. NUMERICAL RESULTS

In this section, numerical results are presented to validate the analysis of NOMA-IE with four-subcarrier subblocks shown in Table II. At the same time, some interesting insights are provided. The average BLER and BER performance of all the considered schemes was evaluated through 10^7 times Monte Carlo simulations. Referred to [20], average channel gains for the FU and NU are $\Omega_F = -6$ dB and $\Omega_N = 0$ dB, respectively. The BPSK scheme is employed for NOMA-IE. Unless otherwise stated, the feasible envelope detection coefficient β_0 is employed at receivers of NOMA-IE.

TABLE IV
THE IM-NOMA MAPPING TABLE FOR $L = 4$ AND $K_u = 2$

Index bits	$\mathbf{I}_u$	subblock $\mathbf{x}_u$
[0, 0]	$\{1, 2\}$	$[s_u(1), s_u(2), 0, 0]^T$
[0, 1]	$\{2, 3\}$	$[0, s_u(1), s_u(2), 0]^T$
[1, 0]	$\{3, 4\}$	$[0, 0, s_u(1), s_u(2)]^T$
[1, 1]	$\{1, 4\}$	$[s_u(1), 0, 0, s_u(2)]^T$

A. Benchmark Schemes

To verify the effectiveness of the proposed NOMA-IE scheme, comparisons are made with conventional OFDM, OFDM-NOMA, and IM-NOMA in the two-user case. The detailed settings are as follows.

- **OFDM**: In this case, the available bandwidth is equally allocated to two users. For a fair comparison with NOMA schemes with the BPSK modulation, 4 amplitude-shift keying (4ASK) modulation is employed, which guarantees the OMA scheme and NOMA schemes are of the same spectral efficiency.
- **OFDM-NOMA**: As in the considered NOMA-IE, BPSK modulation is employed for the NU and the FU. In particular, OFDM-NOMA can be regarded as a special case of the NOMA IE with $L = K_F = K_N$.
- **IM-NOMA**: In this case, the activation patterns of the FU and the NU subblock are independent. We consider $L = 4$, $K_F = K_N = 2$, and the BPSK modulation. The mapping table for the user $u \in \{F, N\}$ is shown in Table IV [12].

B. Validation of Analytical Results

Under different power allocation coefficients, the theoretical BLER and BER of NOMA-IE are verified in Fig. 3 and Fig. 4, respectively. These figures validate the feasibility to express the theoretical BER of the multi-subcarrier subblock by the combination of TSEs. In the high SNR regime, the simulation curves of the FU fit the analytical results quite well. The observation verifies the asymptotic feature of **Approximation 1** and **Approximation 3**. For the NU, there is a small gap between the simulation and the analytical curves even when the SNR is high. This gap is from **Approximation 2** and can be bridged with the increase of the power allocation coefficient a_F as we have discussed.

In addition, error performance under imperfect CSI is shown in both Fig. 3 and Fig. 4. As in [12], the estimated CSI is $\tilde{\mathbf{h}}_u = \mathbf{h}_u + \boldsymbol{\epsilon}$, where $\boldsymbol{\epsilon} \sim \mathcal{CN}(0, \Omega_u v_\epsilon)$ is the channel estimation error, $\Omega_u v_\epsilon$ is the variance of the channel estimation error, and $v_\epsilon \in [0, 1]$. Here we set $v_\epsilon = 0.01$. It can be observed that the imperfect CSI results in the error floor at high SNR. Moreover, the NU has a worse error performance than the FU and hence is more sensitive to the channel estimation error. It can be explained that the perfect SIC process highly relies on exact CSI.

C. Impact of Envelope Detection Coefficient

To show the impact of the value of envelope detection coefficient β_e on the error performance, we plot the average
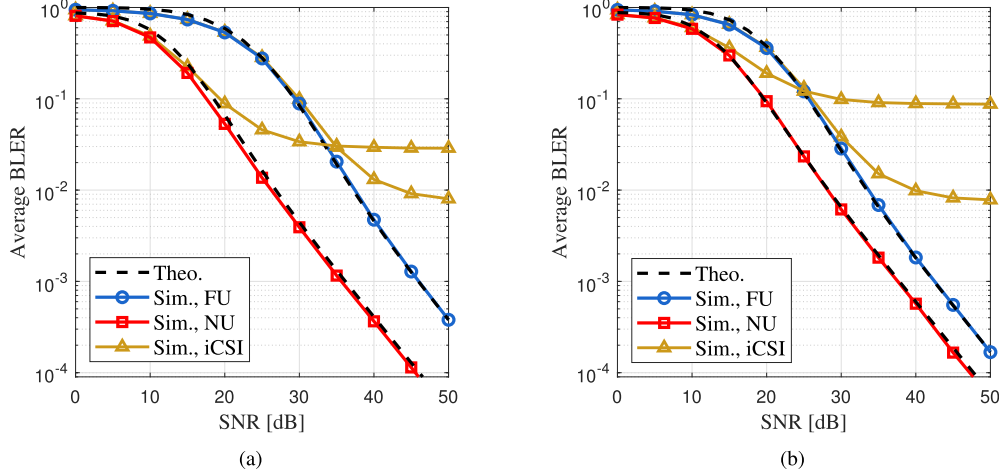
Fig. 3. Average BLER of NOMA-IE under different power allocation coefficients, where "iCSI" denotes imperfect CSI. (a) $a_F = 0.75$, $a_N = 0.25$; (b) $a_F = 0.9$, $a_N = 0.1$.
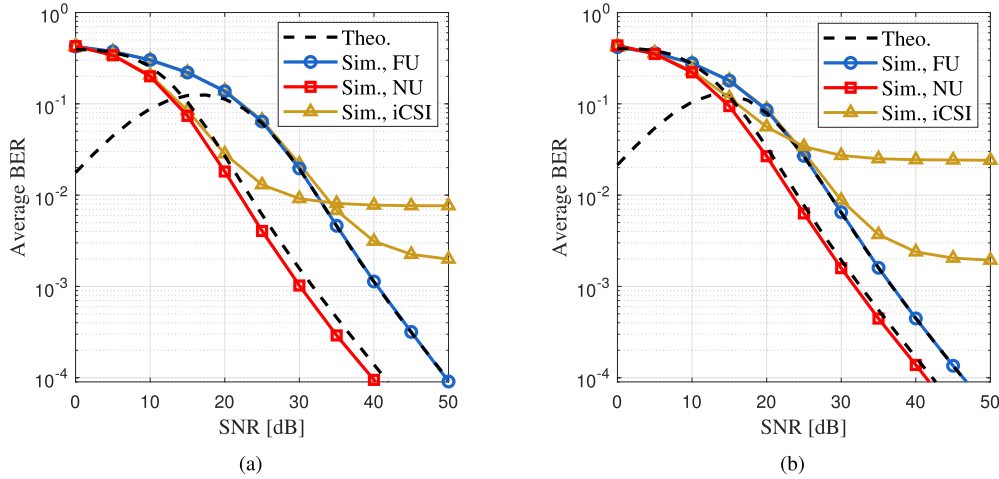

Fig. 4. Average BER of NOMA-IE under different power allocation coefficients, where "iCSI" denotes imperfect CSI. (a) $a_F = 0.75$, $a_N = 0.25$; (b) $a_F = 0.9$, $a_N = 0.1$.

BLER and BER of two users versus β_e with different power allocation coefficients in Fig. 5. In general, with the increase of β_e, the same trend can be found in the curves of both the BLER and BER. The considered error performance is improved to the best first and then decreases. When $a_F = \{0.6, 0.75\}$, both BLER and BER significantly degrade at $\beta_e = 1$. Furthermore, it can be observed that the feasible envelope detection coefficient β_0 obtained in **Corollary 2** always helps to keep the BLER and BER at a low level in the NOMA-IE scheme. We can conclude that in two-user NOMA-IE with BPSK considered, the high error performance is obtained by employing the feasible envelope detection coefficient β_0.

D. Comparisons with OFDM-Based Schemes

In this subsection, we compare the proposed NOMA-IE scheme with the benchmark schemes and illustrate the superiority of the proposed NOMA-IE. The power reallocation policy is employed to guarantee the equal energy efficiency of the considered schemes.

In Fig. 6, we compare the error performance of NOMA-IE with IM-NOMA as a_F grows from 0.5 to 1. As seen from Fig. 6, when $a_F < \tau_F$ the NOMA-IE with the envelope detection coefficient $\beta_e = \beta_0$ considerably outperforms the IM-NOMA. When $a_F > \tau_F$, a slight performance gain can only be obtained at the FU of IM-NOMA. As mentioned previously, $a_F = 0.8$ is the boundary deciding whether the error floor exists for IM-NOMA and NOMA-IE with the conventional detection method, i.e., $\beta_e = 1$. Since the assumption of NOMA-IE (**Assumption 1**) guarantees that the constellations of the superimposed symbols are not overlapped under $a_F > a_N$, we are able to find a detection method to avoid the error floor. That is to say, the design of the NOMA-IE enlarges the feasible range of a_F in the OFDM-IM framework. Therefore, the NOMA-IE has the potential to provide more flexibility for different user requirements. Moreover, with the increase of a_F, the error performance of the FU keeps improving while that of the NU increases first
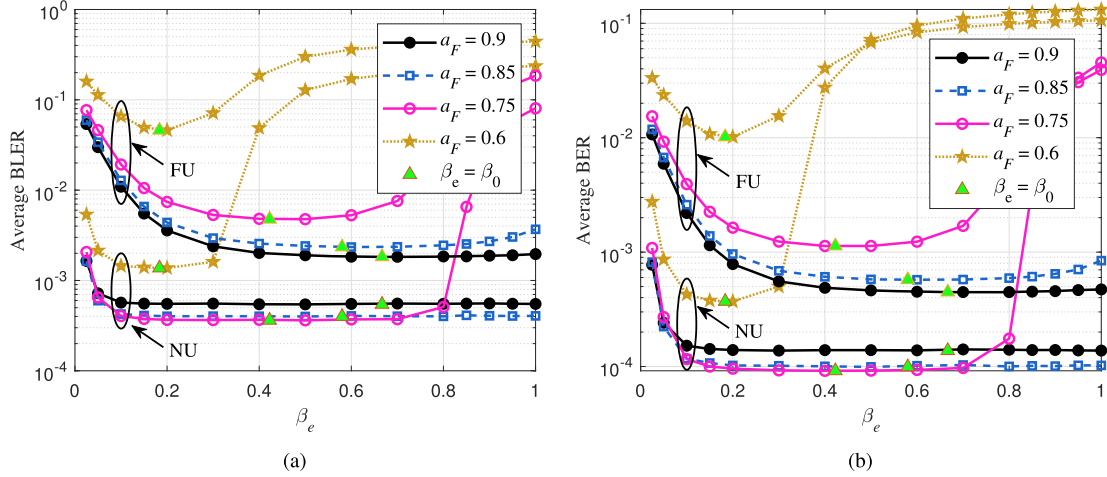
Fig. 5. Error probability versus envelope detection coefficient β_e with different power allocation coefficients. (a) Average BLER; (b) Average BER.
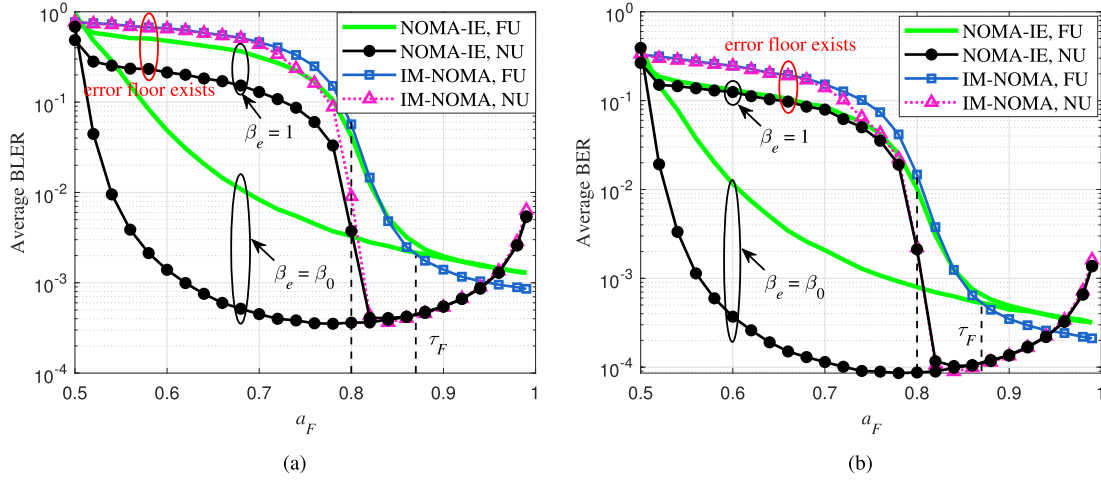

Fig. 6. Error probability of NOMA-IE and IM-NOMA versus power allocation coefficient a_F with SNR = 40 dB. (a) Average BLER; (b) Average BER.

but then decreases. It can be explained that the increase of a_F enlarges the signal difference between two users. However, when a_F is close to one, only low power level is allocated to the NU, and hence the error performance of the NU degrades.

In Fig. 7, we present the BER performance of NOMA-IE, OFDF-NOMA, and conventional OFDM. Compared to OFDM-NOMA and conventional OFDM, 125% extra detection complexity is required for NOMA-IE. However, an obvious performance gain can be achieved by NOMA-IE. From Fig. 7(a), it can be observed that with a BER value lower than 10^{-2}, the proposed NOMA-IE always outperforms the OFDM-NOMA at the same spectral efficiency and energy efficiency. This observation validates the performance gain from the flexibility of the NOMA envelope. Compared with the conventional OFDM, the FU and the NU have better BER performance with $a_F > \tau_F$ and $a_F > \tau_N$, respectively. Therefore, the NOMA-IE with appropriate power allocation coefficients is capable of achieving higher BER performance than the conventional OFDM-based schemes. As shown in Fig. 7(b), up to 5 dB and 8 dB BER gain over OFDM

can be achieved by NOMA-IE at BER of 10^{-4} for the FU and NU, respectively. Another observation is that NOMA-IE outperforms other schemes when the transmit SNR is larger than 25 dB. When SNR is low, the IEE case occurs with a high probability which significantly degrades the error performance of NOMA-IE (**Remark 4**). Therefore, the proposed NOMA-IE is effective especially in the high SNR regime.

E. Performance of Three-User Case

In this subsection, we present the performance of NOMA-IE when more than two users are in a NOMA group. We consider a three-user case, where the average channel gains of U_1, U_2, and U_3 are $\Omega_1 = -6$ dB, $\Omega_2 = -3$ dB, and $\Omega_3 = 0$ dB, respectively. In each four-subcarrier OFDM subblock, we set the number of active subcarriers $K_1 = 4$, $K_2 = 3$, and $K_3 = 2$. Therefore, index bits of U_2 and U_3 are mapped to the envelope according to Table II. Similar to OFDM-NOMA [24], the power allocation coefficients have to fulfill $a_1 > a_2 > a_3$ and $a_1 > a_2 + a_3$ to avoid the constellation overlap.

Fig. 8 illustrates the BER performance of three users under different power allocation setups. We employ the envelope detection coefficient $\beta_e = \frac{\sqrt{a_2} - \sqrt{a_3}}{\sqrt{a_2}}$ for the signal detection of
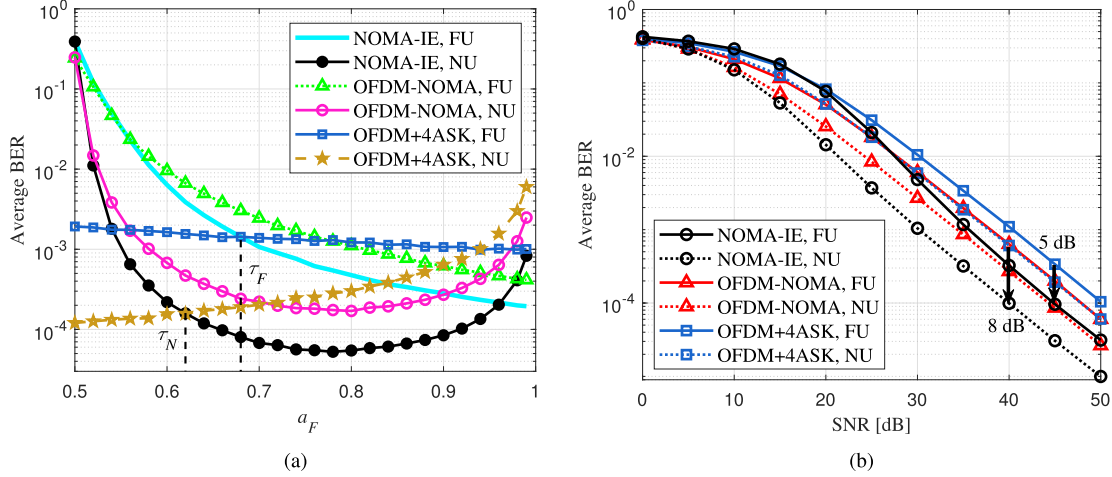
Fig. 7. Comparisons among NOMA-IE, OFDM-NOMA, and OFDM. (a) Average BER versus power allocation coefficient with SNR = 40 dB; (b) Average BER versus SNR with $a_F = 0.9$ and $a_N = 0.1$.
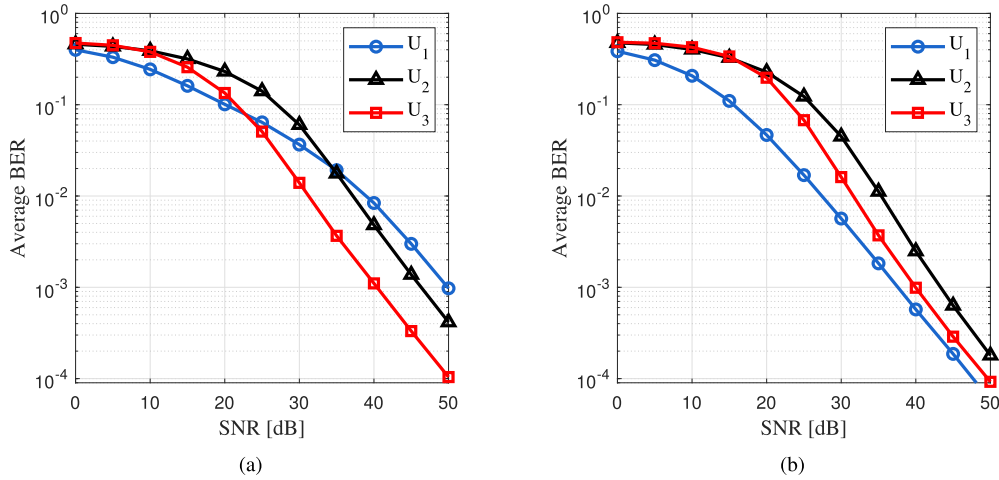

Fig. 8. Average BER of NOMA-IE in the three-user case with $L = K_1 = 4$, $K_2 = 3$, and $K_3 = 2$. (a) $a_1 = 0.7$, $a_2 = 0.2$, and $a_3 = 0.1$; (b) $a_1 = 0.9$, $a_2 = 0.08$, and $a_3 = 0.02$.

U_2. It is shown that with an appropriate β_e, the error floor does not exist under perfect CSI. Therefore, the proposed NOMA-IE scheme is applicable for a NOMA group larger than two. It can be explained that NOMA-IE can be regarded as the mix of OFDM and OFDM-NOMA, and hence the error floor characteristics of NOMA-IE are similar to the two benchmark schemes.

VI. CONCLUSION

In this paper, we have proposed a novel NOMA-IE scheme based on the OFDM-IM framework to explore a new degree of freedom for NOMA. It can be concluded that the envelope is beneficial to NOMA, especially in high SNR regimes. In particular, we have answered three questions listed in Section I to show the benefits of the signal envelope in NOMA. Firstly, the multi-subcarrier subblock can be expressed as the combination of multiple TSEs. Since the theoretical BLER and BER expressions of the TSE are easily obtained, we have derived that of the multi-subcarrier subblock when considering the intra-cluster interference in NOMA. Secondly,

the joint design of the envelope former and the envelope detection coefficient eliminates the error floor, conditioned that the higher power level is allocated to the NU. Lastly, under equal spectral efficiency and energy efficiency, we have shown that the NOMA-IE outperforms the OFDM in terms of error performance when the power allocation coefficient of the NU is larger than a specific threshold. We have also demonstrated that the design of NOMA-IE reduces the intra-cluster interference in NOMA, which improves the error performance of NOMA-IE, especially at high SNR. Future works can focus on the low-complexity detection method, joint design of high-order modulation and channel coding schemes, optimal envelope design, and the applications of NOMA-IE, e.g., applying NOMA-IE in joint radar and communications systems.

REFERENCES

[1] Z. Xie, W. Yi, X. Wu, Y. Liu, and A. Nallanathan, "Exploiting index modulation for enhanced NOMA," in *Proc. IEEE Global Commun. Conf. (GLOBECOM)*, Dec. 2023, accepted.

[2] W. Saad, M. Bennis, and M. Chen, "A vision of 6G wireless systems: Applications, trends, technologies, and open research problems," *IEEE Netw.*, vol. 34, no. 3, pp. 134–142, 2020.

[3] Y. Shao, E. Ozfatura, A. Perotti, B. Popovic, and D. Gündüz, "Attentioncode: Ultra-reliable feedback codes for short-packet communications," *IEEE Trans. Commun.*, Early Access, doi: 10.1109/TCOMM.2023.3280563.

[4] L. Dai, B. Wang, Y. Yuan, S. Han, I. Chih-lin, and Z. Wang, "Non-orthogonal multiple access for 5G: solutions, challenges, opportunities, and future research trends," *IEEE Commun. Mag.*, vol. 53, no. 9, pp. 74–81, 2015.

[5] Z. Ding, Z. Yang, P. Fan, and H. V. Poor, "On the performance of non-orthogonal multiple access in 5G systems with randomly deployed users," *IEEE Signal Process. Lett.*, vol. 21, no. 12, pp. 1501–1505, 2014.

[6] Y. Liu, Z. Qin, M. Elkashlan, Z. Ding, A. Nallanathan, and L. Hanzo, "Nonorthogonal multiple access for 5G and beyond," *Proc. IEEE*, vol. 105, no. 12, pp. 2347–2381, 2017.

[7] Z. Ding, P. Fan, and H. V. Poor, "Impact of user pairing on 5G nonorthogonal multiple-access downlink transmissions," *IEEE Trans. Veh. Technol.*, vol. 65, no. 8, pp. 6010–6023, 2016.

[8] X. Yue, Y. Liu, S. Kang, A. Nallanathan, and Z. Ding, "Exploiting full/half-duplex user relaying in NOMA systems," *IEEE Trans. Commun.*, vol. 66, no. 2, pp. 560–575, 2018.

[9] T. N. Do, D. B. da Costa, T. Q. Duong, and B. An, "Improving the performance of cell-edge users in NOMA systems using cooperative relaying," *IEEE Trans. Commun.*, vol. 66, no. 5, pp. 1883–1901, 2018.

[10] Z. Xie, W. Yi, X. Wu, Y. Liu, and A. Nallanathan, "STAR-RIS aided NOMA in multicell networks: A general analytical framework with gamma distributed channel modeling," *IEEE Trans. Commun.*, vol. 70, no. 8, pp. 5629–5644, 2022.

[11] W. Yi, Y. Liu, A. Nallanathan, and M. Elkashlan, "Clustered millimeter-wave networks with non-orthogonal multiple access," *IEEE Trans. Commun.*, vol. 67, no. 6, pp. 4350–4364, 2019.

[12] E. Başar, Ü. Aygölü, E. Panayırcı, and H. V. Poor, "Orthogonal frequency division multiplexing with index modulation," *IEEE Trans. Signal Process.*, vol. 61, no. 22, pp. 5536–5549, 2013.

[13] E. Basar, "Index modulation techniques for 5G wireless networks," *IEEE Commun. Mag.*, vol. 54, no. 7, pp. 168–175, 2016.

[14] M. Wen, X. Cheng, M. Ma, B. Jiao, and H. V. Poor, "On the achievable rate of OFDM with index modulation," *IEEE Trans. Signal Process.*, vol. 64, no. 8, pp. 1919–1932, 2016.

[15] S. Dang, J. P. Coon, and G. Chen, "Adaptive OFDM with index modulation for two-hop relay-assisted networks," *IEEE Trans. Wireless Commun.*, vol. 17, no. 3, pp. 1923–1936, 2018.

[16] T. Mao, Q. Wang, Z. Wang, and S. Chen, "Novel index modulation techniques: A survey," *IEEE Commun. Surv. Tuts.*, vol. 21, no. 1, pp. 315–348, 2019.

[17] E. Basar, M. Wen, R. Mesleh, M. Di Renzo, Y. Xiao, and H. Haas, "Index modulation techniques for next-generation wireless networks," *IEEE Access*, vol. 5, pp. 16 693–16 746, 2017.

[18] R. Abu-alhiga and H. Haas, "Subcarrier-index modulation OFDM," in *Proc. IEEE Int. Symp. Pers. Indoor Mobile Radio Commun. (PIMRC)*, 2009, pp. 177–181.

[19] K.-H. Kim, "Low-complexity suboptimal ML detection for OFDM-IM systems," *IEEE Wireless Commun. Lett.*, vol. 12, no. 3, pp. 416–420, 2023.

[20] E. Arslan, A. T. Dogukan, and E. Basar, "Index modulation-based flexible non-orthogonal multiple access," *IEEE Wireless Commun. Lett.*, vol. 9, no. 11, pp. 1942–1946, 2020.

[21] A. Almohamad, M. O. Hasna, S. Althunibat, and K. Qaraqe, "A novel downlink IM-NOMA scheme," *IEEE Open J. Commun. Soc.*, vol. 2, pp. 235–244, 2021.

[22] F. Kara and H. Kaya, "BER performances of downlink and uplink NOMA in the presence of SIC errors over fading channels," *IET Commun.*, vol. 12, no. 15, pp. 1834–1844, 2018.

[23] Q. He, Y. Hu, and A. Schmeink, "Closed-form symbol error rate expressions for non-orthogonal multiple access systems," *IEEE Trans. Veh. Technol.*, vol. 68, no. 7, pp. 6775–6789, 2019.

[24] M. Aldababsa, C. Göztepe, G. K. Kurt, and O. Kucur, "Bit error rate for NOMA network," *IEEE Commun. Lett.*, vol. 24, no. 6, pp. 1188–1191, 2020.

[25] H. Yahya, E. Alsusa, and A. Al-Dweik, "Exact BER analysis of NOMA with arbitrary number of users and modulation orders," *IEEE Trans. Commun.*, vol. 69, no. 9, pp. 6330–6344, 2021.

[26] A. Tusha, S. Doğan, and H. Arslan, "A hybrid downlink NOMA with OFDM and OFDM-IM for beyond 5G wireless networks," *IEEE Signal Process. Lett.*, vol. 27, pp. 491–495, 2020.

[27] S. Doğan, A. Tusha, and H. Arslan, "NOMA with index modulation for uplink URLLC through grant-free access," *IEEE J. Sel. Topics Signal Process.*, vol. 13, no. 6, pp. 1249–1257, 2019.

[28] M. B. Shahab, S. J. Johnson, M. Shirvanimoghaddam, M. Chafii, E. Basar, and M. Dohler, "Index modulation aided uplink NOMA for massive machine type communications," *IEEE Wireless Commun. Lett.*, vol. 9, no. 12, pp. 2159–2162, 2020.

[29] Y. Xie, K. C. Teh, and A. C. Kot, "Deep learning-based joint detection for OFDM-NOMA scheme," *IEEE Commun. Lett.*, vol. 25, no. 8, pp. 2609–2613, 2021.

[30] M. Irfan and S. Aïssa, "Generalization of index-modulation: Breaking the conventional limits on spectral and energy efficiencies," *IEEE Trans. Wireless Commun.*, vol. 20, no. 6, pp. 3911–3924, 2021.

[31] D. Cuevas, J. Álvarez Vizoso, C. Beltrán, I. Santamaria, V. Tuček, and G. Peters, "Union bound minimization approach for designing grassmannian constellations," *IEEE Trans. Commun.*, vol. 71, no. 4, pp. 1940–1952, 2023.

[32] M. Chiani, D. Dardari, and M. Simon, "New exponential bounds and approximations for the computation of error probability in fading channels," *IEEE Trans. Wireless Commun.*, vol. 2, no. 4, pp. 840–845, 2003.